

PAPER

Dual-electrode motion artifact cancellation for mobile electroencephalography

To cite this article: Andrew D Nordin *et al* 2018 *J. Neural Eng.* **15** 056024

View the [article online](#) for updates and enhancements.

You may also like

- [Reference layer adaptive filtering \(RLAF\) for EEG artifact reduction in simultaneous EEG-fMRI](#)
David Steyrl, Gunther Krausz, Karl Koschutnig et al.
- [Deep learning for electroencephalogram \(EEG\) classification tasks: a review](#)
Alexander Craik, Yongtian He and Jose L Contreras-Vidal
- [Removal of movement-induced EEG artifacts: current state of the art and guidelines](#)
Dasa Gorjan, Klaus Gramann, Kevin De Pauw et al.

The Breath Biopsy® Guide
Fourth edition

FREE

DOWNLOAD THE FREE E-BOOK

BREATH BIOPSY

OWLSTONE MEDICAL

Dual-electrode motion artifact cancellation for mobile electroencephalography

Andrew D Nordin¹ , W David Hairston² and Daniel P Ferris¹ 

¹ J. Crayton Pruitt Family Department of Biomedical Engineering, University of Florida, Gainesville, FL, United States of America

² U.S. Army Research Laboratory, Human Research and Engineering Directorate, Aberdeen, MD, United States of America

E-mail: andrew.nordin@bme.ufl.edu

Received 22 March 2018, revised 7 July 2018

Accepted for publication 3 August 2018

Published 23 August 2018



Abstract

Objective. Our purpose was to evaluate the ability of a dual electrode approach to remove motion artifact from electroencephalography (EEG) measurements. **Approach.** We used a phantom human head model and robotic motion platform to induce motion while collecting scalp EEG. We assembled a dual electrode array capturing (a) artificial neural signals plus noise from scalp EEG electrodes, and (b) electrically isolated motion artifact noise. We recorded artificial neural signals broadcast from antennae in the phantom head during continuous vertical sinusoidal movements (stationary, 1.00, 1.25, 1.50, 1.75, 2.00 Hz movement frequencies). We evaluated signal quality using signal-to-noise ratio (SNR), cross-correlation, and root mean square error (RMSE) between the ground truth broadcast signals and the recovered EEG signals. **Main results.** Signal quality was restored following noise cancellation when compared to single electrode EEG measurements collected with no phantom head motion. **Significance.** We achieved substantial motion artifact attenuation using secondary electrodes for noise cancellation. These methods can be applied to studying electrocortical signals during human locomotion to improve real-world neuroimaging using EEG.

Keywords: electroencephalography, motion artifact, real-world neuroimaging, signal quality

(Some figures may appear in colour only in the online journal)

1. Introduction

High-density electroencephalography (EEG) scalp electrodes can measure electrical brain activity with high temporal resolution, but the signals are prone to motion artifacts during human movement. Small electrode motions can introduce large magnitude motion artifacts that exceed electrocortical signal magnitudes [1–3]. In addition, varying levels of electromagnetic interference (EMI) can introduce fluctuations in EEG signal magnitude when electrodes move within the surrounding EMI field [4–6].

One method of separating electrocortical signals from EEG data containing motion artifact and other noise signals is blind source separation, such as independent component analysis (ICA) [7]. Although blind source separation approaches have

effectively isolated neural signals from EEG data containing motion artifact, as well as electromyographic (EMG) and electrooculographic artifacts (EOG) [3, 8], these methods are computationally expensive, extremely difficult to implement in real-time, and require some level of calibration or labeling of noise components to work, making them difficult to justify for real-world neuroimaging applications [9]. Post-processing noise identification methods also require the removal of a large number of problematic channels (i.e. retain ~130/248 channels collected [1]), undermining spatial resolution and data reliability across participants and data collections.

Another approach to remove artifacts from scalp EEG recordings is to incorporate alternative sensor measurements into signal cleaning procedures. Simultaneous accelerometer and EEG recordings have been used along with ICA and

filtering to reduce artifacts induced by head motion, while neglecting EMI [10, 11]. During simultaneous EEG recordings and functional magnetic resonance imaging (fMRI), the surrounding magnetic field introduces gradient artifacts that amplify the influence of small head motions [4]. To overcome this problem, researchers have developed dual electrode pairs that concurrently collect artifact biased EEG data, along with the exclusive effects of motion and EMI artifacts, using electrically isolated secondary electrodes [4–6]. This approach has been successful in removing motion artifacts and EMI from dual fMRI and EEG recordings, and holds promise for other types of EEG data collections. Although motion artifact susceptibility depends on the inertial and electrical characteristics of the recording equipment, we have previously shown that cable induced motion artifacts are a major contributor to signal quality declines in the most commonly used system for human mobile EEG studies, BioSemi ActiveTwo hardware [12]. Capturing and removing common artifacts in EEG and isolated noise recordings might therefore allow more effective signal cleaning.

A solution for isolating neural signals from EEG data that could be implemented in real-time is particularly desirable in real-world neuroimaging. It might preserve greater proportions of data and open possibilities for more effective brain computer interfaces [13]. Online de-noising methods, such as spectral subtraction or adaptive filtering, have been applied in speech signal processing and EEG, isolating signals from background noise [13–16]. Fast Fourier Transform and identification of noise-contaminated frequencies provides a computationally low cost solution, but nevertheless requires adaptive noise estimations [13–16]. Simultaneous collection of noise-biased EEG data and isolated noise artifacts could allow signal isolation through spectral subtraction, without assumptions regarding the underlying noise characteristics.

Our purpose was to evaluate the ability of dual electrode hardware and software approaches to remove motion artifacts from scalp EEG. By using a novel array of duplicate EEG electrodes that have a normal scalp electrode combined with a mechanically coupled and inverted noise-only electrode that was electrically isolated from the scalp EEG sensor, we tested the ability of a low computational cost signal processing approach to de-noise scalp EEG data. We used an electrical head phantom and a motion platform to record scalp EEG signals under various motion conditions. We hypothesized that (1) EEG signal quality would decrease at greater movement frequencies; and that (2) EEG recordings using dual electrode pairs would allow effective noise cancellation, greatly improving signal quality during head motion.

2. Methods

2.1. Phantom head and motion platform

We constructed a human head phantom from an adapted mannequin head, using methods outlined in a previous study from our laboratory (figure 1(A)) [17]. Eight dipolar sources were embedded within a dental plaster mixture using eight wire pairs with exposed tips. We used a signal generator to input

artificial neural signals at each source location (USB-3101FS and TracerDAQ software, Measurement Computing, Norton, MA). Each input source consisted of three randomly occurring 500 ms sinusoidal bursts over a 10 s interval, repeated continuously in each trial. Contrasting frequencies were input at each source location (7, 11, 17, 23, 29, 37, 43, 51 Hz, figure 1(B)). Five millivolt input at each source antenna yielded $\pm 12.9 \mu\text{V}$ EEG recording amplitude, depending on electrode location (mean $\pm 3.9 \mu\text{V}$ standard deviation among channels).

Replicating the experimental setup from [17], we generated sinusoidal vertical head motions using a custom motion platform controlled with an electric motor and computer software (dSPACE GmbH, Paderborn, Germany) (figure 1(C)). The phantom head was secured to the motion platform and movements were verified using an 8-camera motion capture system and a marker placed at the base of the phantom head (100 Hz sampling rate, Vicon, Oxford, UK).

2.2. Dual electrode hardware

We assembled a dual electrode array using BioSemi ActiveTwo hardware (Amsterdam, Netherlands). The system relies on active electrodes that are less susceptible to motion and EMG artifacts compared to passive electrodes, though the system is prone to cable induced motion artifacts [17]. Our dual electrode array consisted of eight scalp electrodes recording normal EEG and 8 mechanically coupled and inverted secondary electrodes that were electrically isolated from the scalp EEG sensors, recording only motion artifacts and electrical noise, without artificial neural signals (figure 2(B)). Dual electrodes were fixed to one another using double-sided adhesive, with wires secured using electrical tape (figure 2(B)). Pin-Type Active-electrodes were used for recording normal scalp EEG signals (figures 2(A) and 3(A)) and inverted Flat-Type Active-electrodes were used for recording noise (figures 2(B) and 3(B)). Data were collected using two electrically independent, daisy-chained, BioSemi ActiveTwo AD-boxes (512 Hz sampling rate), with separate reference and ground electrodes for each system (CMS and DRL, respectively). Data were therefore temporally synced and acquired in a single file. The electrically isolated noise electrodes were connected via a conductive stretch fabric (4900 Stretch Conductive Fabric, Holland Shielding Systems BV, Dordrecht, Netherlands) serving as a synthetic outer ‘skin’ layer overlaid on the primary cap and EEG sensors (figure 3(C)). The combined resistance of the dental plaster and standard multi-purpose conductive gel (Signa gel, Parker Laboratories Inc., Fairfield, NJ, USA) was compared to ensure it approximately matched that of the conductive gel and fabric using a multi-meter. Our testing showed agreement with Kline *et al* [2] (~ 0.9 Mohm), approximately simulating the resistance of the human scalp (~ 0.001 – 0.1 Mohm for dry skin [18]).

2.3. EEG preparation

During scalp EEG preparation, we placed an appropriately sized cap on the phantom head and injected conductive gel at each electrode site. Pin-Type electrodes were inserted into

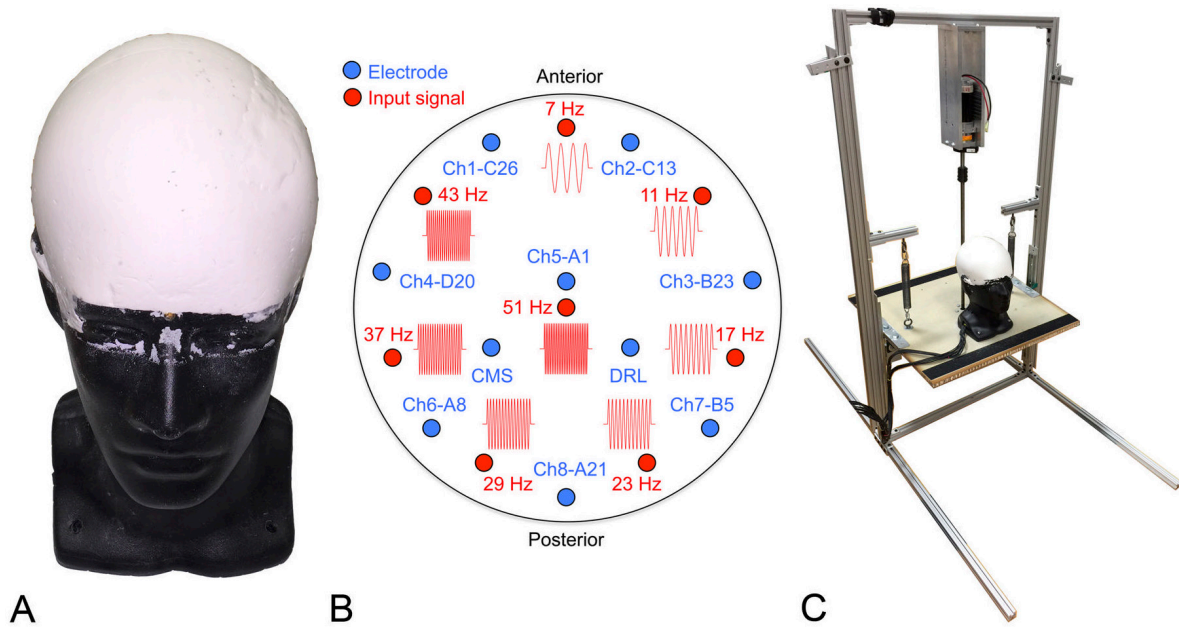


Figure 1. (A) Phantom human head, (B) artificial neural source locations, frequency content, and scalp EEG electrode locations, (C) motion platform.

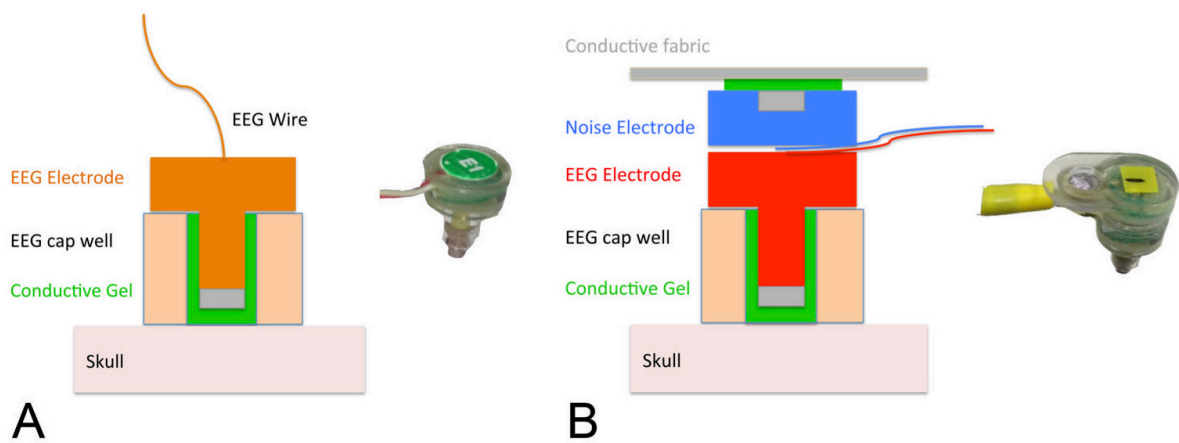


Figure 2. (A) BioSemi Active Pin Type electrode, (B) custom dual electrode pair (BioSemi Active Pin Type electrode and inverted Flat Type electrode).

eight locations on a standard 128-channel cap (Electro-Cap International, Inc., Eaton, OH, USA) (figures 1(B) and 3(B)). The CMS and DRL electrodes were placed on locations specified by BioSemi (figures 1(B) and 3(B)). After inserting each Pin-Type electrode, we overlaid the secondary cap and injected conductive gel between the inverted Flat-Type electrode and conductive fabric (figure 3(C)). This replicates the intended use of Flat-Type BioSemi ActiveTwo electrodes, which typically lay flat against the skin with a small pocket of gel bridged to the Ag/AgCl recording pellet. Here, the conductive fabric served as an artificial skin circuit, with noise data recorded independently from the scalp EEG. Following BioSemi guidelines (www.biosemi.com), we checked scalp EEG and noise electrode offsets, ensuring <20 mV was observed at each channel. Electrode wires exiting the secondary cap were bundled using Velcro straps and connected to each respective BioSemi ActiveTwo system box.

As a means of comparing our dual electrode setup to a standard scalp EEG preparation, we repeated the experimental procedure on a separate day using eight standard Pin-Type electrodes at the same relative locations (figure 3(A)).

2.4. Experimental protocol

To investigate the effects of motion artifact on scalp EEG we used sinusoidal vertical motions at contrasting movement frequencies (stationary, 1.00, 1.25, 1.50, 1.75, and 2.00 Hz), with consistent amplitude across conditions (approximately 3.5 cm). In each condition, we simultaneously recorded scalp EEG data and noise from secondary electrodes for 300s. Prior to motion conditions, we recorded baseline noise captured by each set of electrodes without input signals. Next, we recorded EEG data with artificial neural inputs while stationary, providing ground-truth measures for comparison.

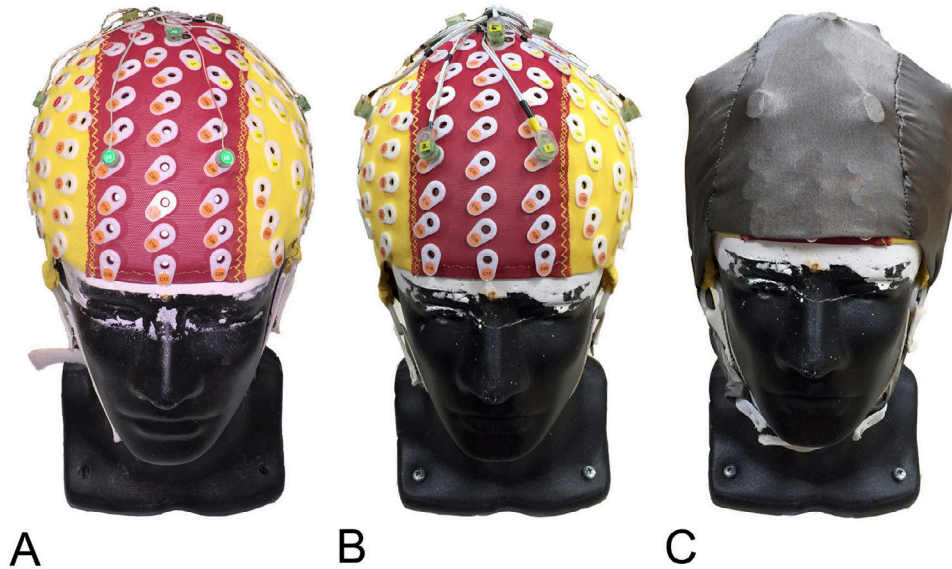


Figure 3. (A) standard scalp EEG setup, (B) dual electrode array, (C) overlaid conductive secondary cap.

The same procedure was followed for each motion condition, recording baseline noise plus motion artifact prior to recording artificial neural data during movement. Because our dual electrode setup used an overlaid secondary cap that may reduce motion artifacts caused by electrode and cable motions [19], we repeated the experimental procedure using a standard EEG preparation, thus providing two parallel datasets (dual electrode and standard electrode, respectively).

2.5. Data analysis-signal quality

To quantify signal quality, we computed signal-to-noise ratio (SNR), time series cross-correlation, and root mean square error (RMSE) for each scalp electrode, in each motion condition. Signal-to-noise ratios were computed from the root mean square of the respective scalp EEG and noise signals (dB, $20\log_{10}(\text{EEG}/\text{noise})$). EEG signals for calculating SNR were recorded without motion and noise signals were recorded from each scalp electrode when the artificial neural inputs were turned off and each motion condition was repeated. Cross-correlations and RMSE (μV) were computed for each scalp electrode by comparing ground-truth measurements recorded while stationary to recordings in each motion condition. Greater signal quality was associated with greater SNR and cross correlation, and lesser RMSE.

2.6. Data analysis-artifact attenuation

Our second aim was to evaluate the ability of dual electrode hardware and software approaches to remove motion artifacts from scalp EEG data. To achieve this goal, we used sliding window spectral subtraction, removing noise signals from scalp EEG data captured by secondary electrodes (figure 4). Because our dual electrodes were secured to one another, we hypothesized these electrode pairs would experience equivalent motions and electrical noise, thus allowing noise cancellation. Spectral subtraction was implemented after high-pass filtering scalp EEG and noise data at 0.8 Hz

(EEGLAB 13.5.4b) [20]. We then used custom MATLAB scripts (R2015b, Natick, MA, USA) to implement a 500 ms Hamming window with 94% overlap, followed by Fast-Fourier Transform (FFT). Because the lowest artificial neural input frequency was 7 Hz, we used a 500 ms window length to accurately detect a minimum frequency of 2 Hz (4 Hz for two times Nyquist frequency), though extended window lengths can improve low frequency representations. To cancel motion artifacts, we set EEG frequencies to zero if the noise frequency exceeded ten times the median noise FFT coefficient value (figure 4). To cancel electrical noise, we set EEG frequencies to zero if they were below ten times the median noise FFT coefficient value (figure 4). We applied these criteria separately to the real and imaginary portions of the signal, prior to reconstruction using inverse FFT (figure 4). Separately treating the real and imaginary portions of the signal limited distortion compared to cancelling both real and imaginary signal components together.

2.7. Statistical analysis

We evaluated changes in signal quality among experimental setup and motion conditions using separate 3×6 repeated measures ANOVAs ($\alpha = 0.05$) performed on the 8-channel EEG data for each signal quality measure (SNR, cross-correlation, and RMSE) (IBM SPSS Statistics, Armonk, NY, USA). Experimental setup conditions included a standard scalp EEG preparation (standard electrode), dual electrode scalp EEG data with an overlaid secondary cap prior to noise cancellation (secondary cap), and dual electrode scalp EEG data after noise cancellation (noise cancellation). Before computing cross-correlation statistical comparisons across conditions, r -values were converted to z -scores using the Fisher z -transform. Because cross correlation comparisons were made in comparison to the stationary condition, z -scores in the stationary condition ($r = 1.00$) were instead set to 3. Following significant statistical interaction, simple main effects analyses were performed. Huynh-Feldt adjustments

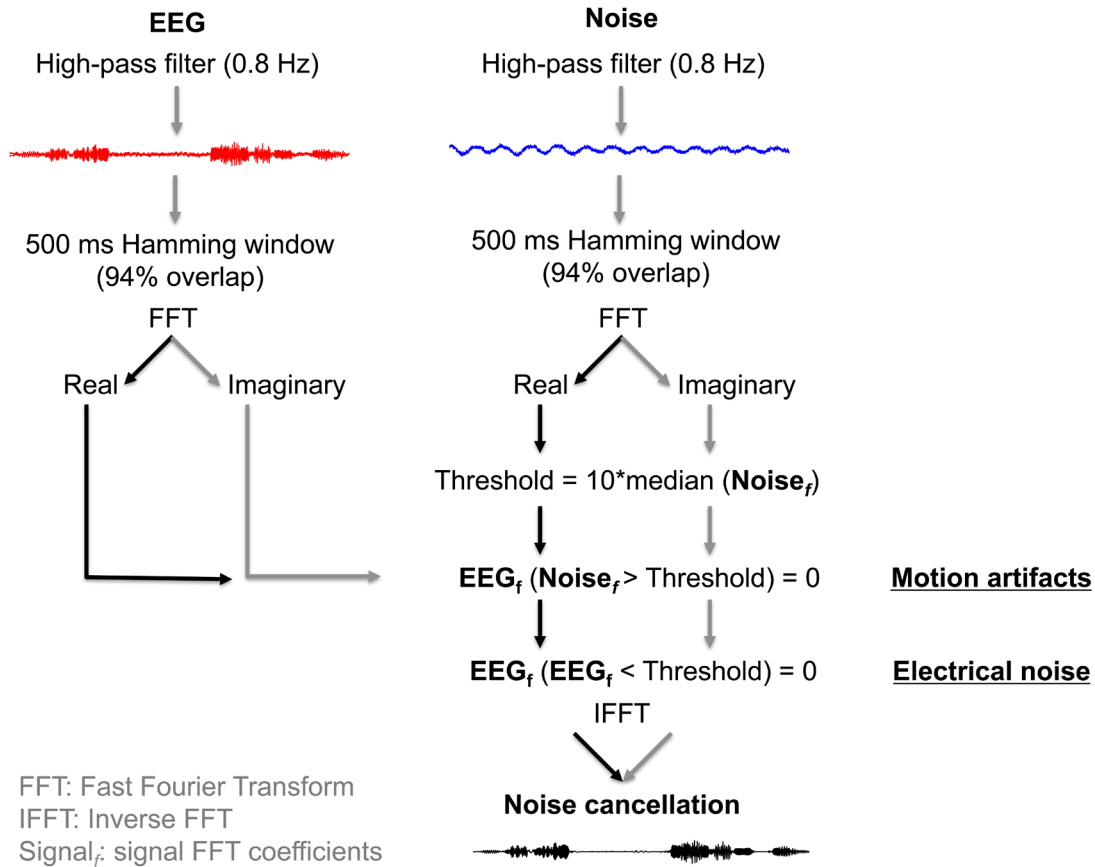


Figure 4. Dual electrode signal processing approach. Noise electrodes were used to cancel large magnitude motion artifacts ($>$ Threshold) and low magnitude electrical noise ($<$ Threshold) from the EEG electrodes. The noise cancellation threshold was computed from the median FFT coefficient value in each 500 ms window.

were used following sphericity violations and Bonferroni corrections were used for multiple comparisons [21].

3. Results

On average, phantom head movement amplitude was 3.4 ± 0.2 cm among conditions, measured from motion capture data. Exemplar time series and power spectra data show secondary electrodes captured motion artifacts at the movement frequency, as well as background electrical noise (figures 5(A) and (B)). In general, spectral power at the artificial neural input frequencies (7, 11, 17, 23, 29, 37, 43, and 51 Hz) was maintained after subtraction, depending on sensor location relative to transmitting antenna, but was attenuated outside this portion of the spectrum (figure 5(B)), resulting in cleaner time series data (figure 5(A)). Signal quality improved following noise cancellation when compared to standard EEG measurements and after securing electrodes and wires with a secondary cap (figures 6(A)–(C)). Standard scalp EEG recordings showed the largest decline in signal quality at higher movement frequencies (figures 6(B) and (C)).

3.1. Signal-to-noise ratio

SNR was influenced by the interaction of movement frequency and setup ($F_{(10,70)} = 9.0$, $p < 0.001$, $\eta^2 = 0.56$; figure 6(A)).

At 2.00 Hz motion, SNR decreased slightly in each setup (standard electrode: $F_{(1.1,7.5)} = 15.2$, $p = 0.005$, $\eta^2 = 0.68$; secondary cap: $F_{(5,35)} = 15.2$, $p < 0.001$, $\eta^2 = 0.84$; noise cancellation: $F_{(5,35)} = 12.3$, $p < 0.001$, $\eta^2 = 0.64$; figure 6(A), pairwise comparisons: $p \leq 0.046$). In each motion condition, SNR after noise cancellation exceeded standard electrode and secondary cap conditions (pairwise comparisons: $p < 0.001$; figure 6(A)).

3.2. Cross-correlation

Cross-correlation was influenced by the interaction of movement frequency and setup ($F_{(10,70)} = 40.4$, $p < 0.001$, $\eta^2 = 0.85$; figure 6(B)). During motion, cross-correlation decreased relative to stationary in each setup (standard electrode: $F_{(1.4,9.6)} = 211.7$, $p < 0.001$, $\eta^2 = 0.97$; secondary cap: $F_{(1.1,7.9)} = 607.0$, $p < 0.001$, $\eta^2 = 0.99$; noise cancellation: $F_{(2.1,15.3)} = 392.1$, $p < 0.001$, $\eta^2 = 0.98$; figure 6(B)) and at 2.00 Hz motion frequency in the standard setup (pairwise comparisons: $p \leq 0.018$; figure 6(B)). In each motion condition, cross-correlation after noise cancellation exceeded standard electrode and secondary cap conditions (pairwise comparisons: $p \leq 0.004$; figure 6(B)). At 2.00 Hz motion, cross-correlation after noise cancellation exceeded both secondary cap and standard electrode conditions ($p < 0.001$; figure 6(B)).

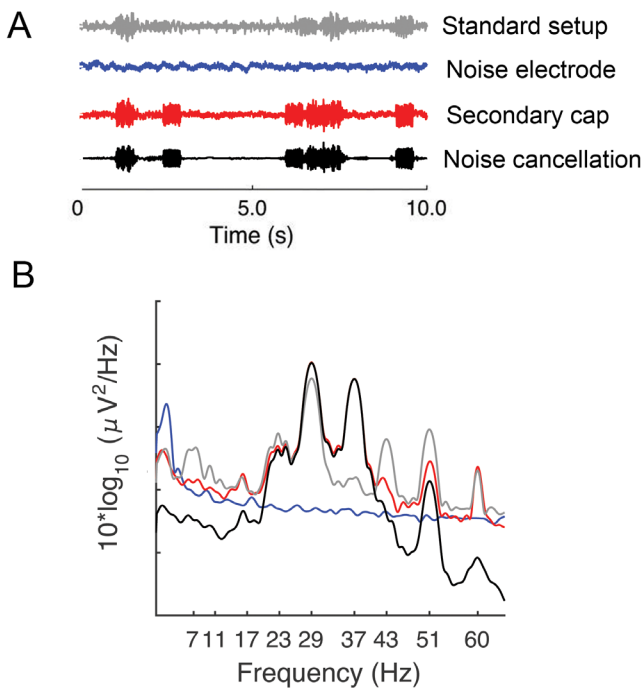


Figure 5. (A) Exemplar electrode time series EEG data during 2.0 Hz motion. Data were high-pass filtered at 0.8 Hz. (B) Corresponding electrode power spectra showing peaks at the artificial neural input frequencies and the effects of motion artifact.

3.3. Root mean square error

Root mean square error was influenced by the interaction of movement frequency and setup ($F_{(10,70)} = 11.5$, $p < 0.001$, $\eta^2 = 0.62$; figure 6(C)). In each setup, RMSE increased relative to stationary (standard electrode: $F_{(1.0,7.2)} = 23.0$, $p = 0.002$, $\eta^2 = 0.77$; secondary cap: $F_{(1.3,9.1)} = 1900.8$, $p < 0.001$, $\eta^2 = 1.00$; noise cancellation: $F_{(1.3,9.0)} = 222.2$, $p < 0.001$, $\eta^2 = 0.97$; figure 6(C)) and increased at 2.00 Hz movement frequency in the standard EEG setup (pairwise comparisons: $p \leq 0.015$). In each motion condition, RMSE after noise cancellation was reduced relative to the secondary cap and standard setup conditions (pairwise comparisons: $p \leq 0.008$; figure 6(C)). RMSE in the secondary cap condition was also less than the standard setup at 1.00, 1.75, and 2.00 Hz movement frequencies (pairwise comparisons: $p \leq 0.047$).

4. Discussion

Our results show decreased signal quality in standard EEG recordings during motion, particularly at greater movement frequency. Although securing electrodes and wires with a secondary cap minimized signal loss, active noise cancellation using sliding window spectral subtraction from dual electrode pairs restored signal quality during motion when compared to ground-truth stationary recordings. Our experimental approach relied on an electrical head phantom device and robotic motion platform, which allowed us to compare the effects of motion artifact on scalp EEG while limiting confounding sources of variation, including inter and intra-subject variability, as well as biological artifacts (i.e. eye and

muscle artifacts). These methods provided the experimental control necessary for establishing hardware and software benchmarks prior to human testing [9, 17].

In line with our aims, secondary electrodes captured the movement frequency of the motion platform, with limited contributions at greater harmonics that were observed by Kline *et al* [2] and Gwin *et al* [8]. The harmonics in these previous studies were likely related to individual cable motions that were not bundled [21]. Additional harmonics of the motion platform were sometimes visible in the standard electrode setup, but not the secondary cap or noise cancellation conditions (figure 5(B)). In agreement with Reis *et al* [22], as well as Nathan and Contreras-Vidal [19], who reported motion artifact suppression using a double-layer stretchable mesh cap overlaying electrodes and cables, we observed limited motion artifacts across movement frequencies with the use of a secondary cap and secured cables (figures 5 and 6). The additional benefits of our conductive cap were demonstrated after noise cancellation, providing a reference layer that captured the exclusive effects of motion artifact and background electrical noise. Although the secondary cap and noise cancellation conditions showed small but statistically significant decreases in SNR at 2.00 Hz movement frequency (figure 6(A)), signal quality decreased most dramatically in the standard electrode setup and this was not overcome by securing electrodes and cables alone (figures 6(B) and (C)).

Previous studies have made attempts at quantifying motion artifacts captured by scalp EEG using a head-mounted accelerometer during human walking [10, 23]. Daly *et al* [10] and Onikura and Iramina [11] demonstrated artifact removal using an accelerometer-based template and filtering of ICs extracted during head movements. Kline *et al* [2], however, showed artifact complexity exceeded that measured by a single head-mounted accelerometer during walking. The use of individual accelerometers located at each scalp electrode may provide an improved motion artifact template [24], though this approach fails to capture the effects of cable motions, as well as signal fluctuations arising from the surrounding EMI field [4, 6]. Our use of secondary electrodes limited the need to model movement induced artifacts and electrical noise, reducing the computational cost and difficulty of artifact removal. Emerging real time signal processing approaches may therefore benefit from improved noise templates measured from secondary electrodes. Recently, Nathan and Contreras-Vidal [19] applied Artifact Subspace Reconstruction (ASR) [25] to scalp EEG during walking, which implements sliding window subspace decomposition using principal component analysis (PCA). ASR has been used for removing eye, muscle, and motion artifacts [26], cleaning portions of noisy data that deviate from baseline, while relying on estimates of clean versus noisy data. Kilicarslan *et al* [24] outlined an alternative approach for removing eye artifacts from scalp EEG, implementing adaptive (H^∞) filtering using reference electrooculographic (EOG) electrodes. This real time approach outperformed both traditional ICA and ASR, particularly for local disturbances, suggesting online signal processing approaches that make use of secondary electrode measurements can improve scalp EEG de-noising procedures.

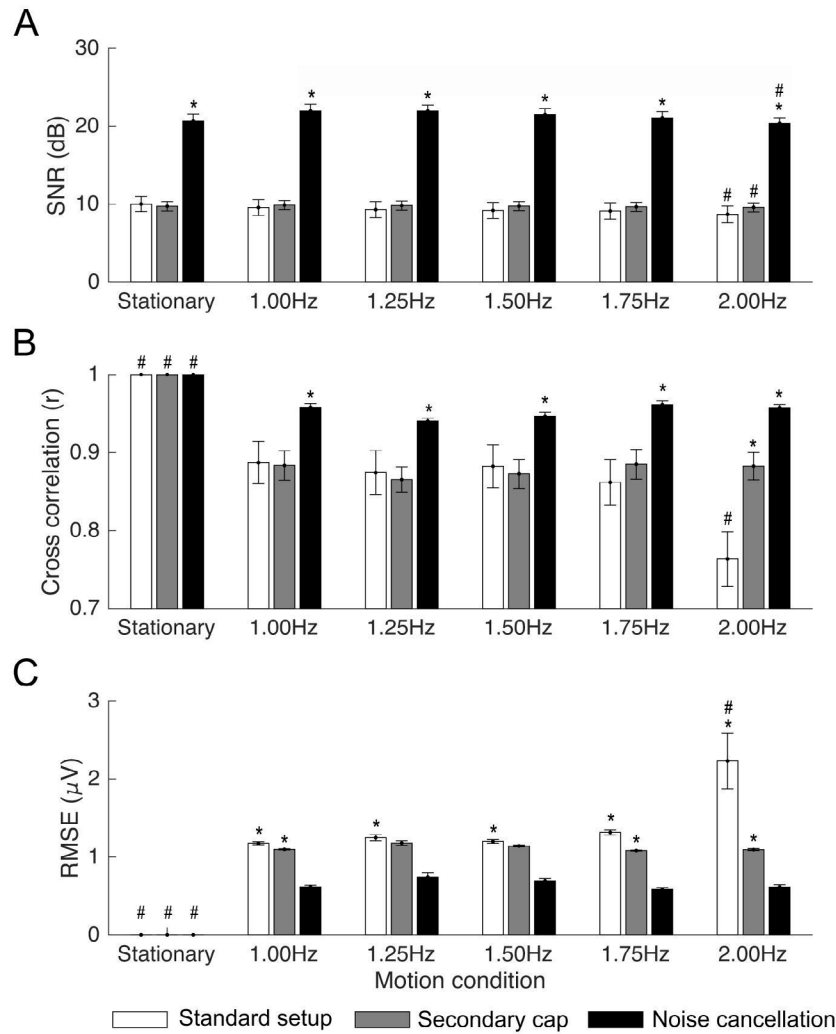


Figure 6. Signal quality summaries in each setup and motion condition (8-electrode mean \pm standard error). (A) Signal-to-noise ratio, (B) cross correlation, (C) root mean square error (RMSE) (*: significant setup differences by motion condition, #: significant motion condition differences by setup, pairwise comparisons: $p < 0.05$).

There were limitations in our study that impact our interpretations. Our signal processing approach relied on spectral noise cancellation applied to artificial neural signals with known frequency content independent of the robotic platform movement frequencies. Although electrode and cable motions can introduce frequency harmonics, our setup may have limited their appearance [19]. Overlap among motion artifacts and neural signals may undermine spectral cancellation, attenuating both motion artifacts and neural signals, though this can be partially overcome using materials with electrical properties that better match the human scalp, enabling straightforward spectral subtractions. Notably, secondary electrodes were more sensitive to motion artifacts than normal scalp electrodes, as observed in the time series magnitudes and spectral power at the movement frequency (figures 5(A) and (B), respectively), which can be attributed to the low surface resistivity of the conductive fabric. Nevertheless, we maintained signal quality after noise cancellation (figure 6), detecting spectral peaks at the artificial neural input frequencies. Although reduced absolute spectral power was observed below 17 Hz after subtraction (figure 5(B)), this trend was

dependent on scalp electrode location relative to the transmitting antennas. Further, we chose a relatively aggressive threshold for cancelling motion artifacts and defining our noise floor in this case, while separate high (motion artifact) and low (electrical noise floor) thresholds could be used to tune the performance of our algorithm. Prior to noise cancellation, differences in spectral power between standard and dual electrode datasets can be attributed to alterations in phantom head conductivity over time. Because we collected these datasets approximately one-week apart, we performed signal quality assessments from the stationary condition in each respective setup to serve as a relative baseline, thus negating these differences.

Our investigation was restricted to phantom human head testing during robotically controlled vertical sinusoidal motions, with acknowledged tradeoffs between experimental control and ecological relevance. Because vertical head accelerations have shown the strongest correlation with EEG motion artifacts during walking ($0.4\text{--}1.6\text{ m s}^{-1}$), we exclusively examined vertical head movements [2]. Electrode motions, however, differ across scalp locations and are not limited to

the vertical direction, nor are they strictly sinusoidal [2, 27]. Prior investigations have relied on *post hoc* comparisons of previously processed data without knowledge of the ground truth neural signals, limiting interpretations about the influence of signal processing procedures on neural versus artifact components. Our approach overcame this limitation, with admitted restrictions surrounding the use of a dental plaster mold as a surrogate for a human head. With this in mind, we are continuing to quantify the electrical properties of our phantom heads, while also investigating alternative materials that better match electrical and mechanical characteristics of human tissue [28]. In any case, establishing benchmarks for scalp EEG hardware and software is an essential step for overcoming the effects of motion artifacts that currently limit our understanding of human brain dynamics during movement.

5. Conclusion

Our combined hardware and software approach reduced motion artifacts captured by scalp EEG during vertical head motions. Assembly of a dual electrode array that captured neural signals and motion artifacts from normal scalp electrodes, along with electrically isolated, mechanically coupled secondary electrodes that exclusively captured noise, allowed noise cancellation and the recovery of ground truth artificial neural signals. Benchmark testing these methods using an electronic phantom human head and robotic motion platform demonstrated substantially improved signal quality during movement. These methods could be used in EEG recordings during human movement to improve real-world neuroimaging capabilities.

Acknowledgments

We thank Bryan Schlink for his data collection assistance. This research was supported by the Cognition and Neuroergonomics Collaborative Technology Alliance ARL W911NF-10-2-0022.

ORCID iDs

Andrew D Nordin  <https://orcid.org/0000-0001-8340-7815>
Daniel P Ferris  <https://orcid.org/0000-0001-6373-6021>

References

- [1] Gwin J T, Gramann K, Makeig S and Ferris D P 2011 Electrocortical activity is coupled to gait cycle phase during treadmill walking *NeuroImage* **54** 1289–96
- [2] Kline J E, Huang H J, Snyder K L and Ferris D P 2015 Isolating gait-related movement artifact in electroencephalography during human walking *J. Neural Eng.* **12** 1–16
- [3] Snyder K L, Kline J E, Huang H J and Ferris D P 2015 Independent component analysis of gait-related movement artifact recorded using EEG electrodes during treadmill walking *Front Hum. Neurosci.* **9** 639
- [4] Chowdury M E, Mullinger K J and Bowtell R 2015 Simultaneous EEG-fMRI: evaluating the effect of the cabling configuration on the gradient artefact *Phys. Med. Biol.* **60** 241–50
- [5] Chowdury M E, Mullinger K J, Glover P and Bowtell R 2013 Reference layer artefact subtraction (RLAS): a novel method of minimizing EEG artefacts during simultaneous fMRI *NeuroImage* **84** 307–19
- [6] Jorge J, Grouiller F, Gruetter R, van der Zwaag W and Figueiredo P 2015 Towards high-quality simultaneous EEG-fMRI at 7 T: detection and reduction of EEG artifacts due to head motion *NeuroImage* **120** 143–53
- [7] Uriguen J A and Garcia-Zapirain B 2015 EEG artifact removal-state-of-the-art and guidelines *J. Neural Eng.* **12** 031001
- [8] Gwin J T 2010 Removal of movement artifact from high-density EEG recorded during walking and running *J. Neurophysiol.* **103** 3526–34
- [9] McDowell K et al 2013 Real-world neuroimaging technologies *IEEE Access* **1** 131–49
- [10] Daly I, Billinger M, Scherer R and Muller-Putz G 2013 On the automated removal of artifacts related to head movement from the EEG *IEEE Trans. Neural Syst. Rehabil. Eng.* **21** 427–34
- [11] Onikura K and Iramina K 2015 Evaluation of a head movement artifact removal method for EEG considering real-time processing *Proc. 8th Biomed. Eng. Int. Conf. (BMEiCON)* pp 1–4
- [12] Symeonidou E-R, Nordin A D, Hairston W D and Ferris D P 2018 Effects of cable sway, electrode surface area, and electrode mass on electroencephalography signal quality during motion *Sensors* **18** 1073
- [13] Alhaddad M J, Kamel M I, Makary M M, Hargas H and Kadah Y M 2014 Spectral subtraction denoising preprocessing block to improve P300-based brain-computer interfacing *Biomed. Eng. Online* **13** 36
- [14] Mihajlovic V, Li H, Grundlehner B, Penders J and Schouten A C 2012 Investigating the impact of force and movements on impedance magnitude and EEG *Proc. Annu. Int. Conf. IEEE Eng. Med. Biol. Soc.* pp 1466–9
- [15] Mihajlovic V, Patki S and Grundlehner B 2014 The impact of head movements on EEG and contact impedance: an adaptive filtering solution for motion artifact reduction *Proc. Annu. Int. Conf. IEEE Eng. Med. Biol. Soc.* pp 5064–7
- [16] Vaseghi S V 2000 Spectral subtraction *Advanced Digital Signal Processing and Noise Reduction* 2nd edn (West Sussex: Wiley) pp 333–54
- [17] Oliveira A S, Schlink B R, Hairston W D, Konig P and Ferris D P 2016 Induction and separation of motion artifacts in EEG data using a mobile phantom head device *J. Neural Eng.* **13** 036014
- [18] Fish R and Geddes L A 2003 *Medical and Bioengineering Aspects of Electrical Injuries* (Tucson: Lawyers & Judges Publishing Company, Inc.)
- [19] Nathan K and Contreras-Vidal J L 2015 Negligible motion artifacts in scalp electroencephalography (EEG) during treadmill walking *Front. Hum. Neurosci.* **9** 708
- [20] Delorme A and Makeig S 2004 EEGLAB: an open source toolbox for analysis of single-trial EEG dynamics including independent component analysis *J. Neurosci Methods* **134** 9–21

- [21] Field A 2009 *Discovering Statistics Using SPSS* 3rd edn (Thousand Oaks, CA: SAGE Publications Ltd.)
- [22] Reis P M R, Hebenstreit F, Gabsteiger F, von Tscharnher V and Lochmann M 2014 Methodological aspects of EEG and body dynamics measurements during motion *Front. Hum. Neurosci.* **8** 156
- [23] Castermans T, Duvinage M, Cheron G and Dutoit T 2014 About the cortical origin of the low-delta and high-gamma rhythms observed in EEG signals during treadmill walking *Neurosci. Lett.* **561** 166–70
- [24] Kilicarslan A, Grossman R G and Contreras-Vidal J L 2016 A robust adaptive denoising framework for real-time artifact removal in scalp EEG measurements *J. Neural Eng.* **13** 026013
- [25] Mullen T *et al* 2013 Real-time modeling and 3D visualization of source dynamics and connectivity using wearable EEG *Proc. Annu. Int. Conf. IEEE Eng. Med. Biol. Soc.* pp 2184–7
- [26] Bulea T C, Kim J, Damiano D L, Stanley C J and Park H-S 2015 Prefrontal, posterior parietal and sensorimotor network activity underlying speed control during walking *Front. Hum. Neurosci.* **9** 247
- [27] Costa A, Salazar-Varas R, Ubeda A and Azorin J M 2016 Characterization of artifacts produced by gel displacement on non-invasive brain-machine interfaces during ambulation *Front. Neurosci.* **10** 60
- [28] Hairston W D, Slippher G A and Yu A 2016 Ballistic gelatin as a putative substrate for EEG phantom devices (arXiv:1609.07691)